Experimental considerations on the determination of radiation fields in an electron accelerator

L. Mondragón-Contreras, F. J. Ramírez-Jiménez, J. M. García-Hernández, M. A. Torres Bribiesca,
R. López Callejas, and R. Peña Eguiluz
Instituto Nacional de Investigaciones Nucleares, Departamento de Sistemas Electrónicos,
Carretera México-Toluca s/n, La Marquesa, Ocoyoacac, Estado de México, 52750, México.
Instituto Tecnólogico de Toluca,
Av. Tecnológico S/N, Ex Rancho la Virgen, Metepec, 52140, Estado de México, México.

The determination of the different radiation fields in an electron accelerator requires the use of selected radiation detectors, in this work we describe the experimental considerations on the determination of the intensity of electrons and X-rays generated by bremsstrahlung in an experimental electron accelerator covering the energy range from 80 keV to 485 keV. A lithium- drifted silicon detector, a high-purity germanium detector, a scintillation detector and a PIN diode were used in the experiments. Spectroscopic measurements allowed us to verify the terminal voltage of the accelerator. The PIN photodiode can measure the intensity of X-rays produced, with this information, we could determine its relationship with both the electron beam current and the accelerating voltage of the accelerator.

1. Introduction

The capacity of high energy electrons and photons to break chemical bonds and to release free active radicals on different materials, has led to important industrial applications of these kinds of beams such as: improvement of the properties of polymers [1,2], sterilization of medical instruments and supplies, disinfection of cosmetics or preservation of food [3]. The necessary radiation to carry out these processes can be obtained from nuclear decay of radioactive materials like ^{60}Co or ^{137}Cs, which are used to irradiate products that require high dose rates and high penetration, or from electron accelerators that are used mainly in applications requiring superficial high doses [4,5].

The Nuclear Research National Institute of México (ININ) has an Experimental Pelletron Electron Accelerator, which produces electron beams with current intensities from 1 μA to 10 μA. In these experiments the accelerating voltage was adjusted from 80 kV to 485 kV; the electron beam passes through a 40 μm titanium window and afterwards it collides with a 3 mm aluminum target, the interaction of the electrons with the window and the target produces X-rays (bremsstrahlung) [6].

The X-ray intensity produced by bremsstrahlung effect is measured by using an easy to implement X-ray monitor built with a PIN photodiode applied as a radiation detector [7].

2. Intensity of X-Rays

The X-rays generated by the electron accelerator can be evaluated by means of the intensity of X-rays that is defined as:

$$I_x = N_p E_p \qquad (1)$$

where: N_p is the number of photons per second (s^{-1}) and per unit of area (cm^{-2}), E_p is the photon energy (keV). The intensity of X-rays is directly related with the power of the X-rays.

3. Experimental setup

The Experimental Pelletron Electron Accelerator produces electron beams with current intensities from 1 μA to 10 μA. In these experiments the accelerating voltage was adjusted from 80 kV to 485 kV; the electron beam passes through a 40 μm titanium window and afterwards it collides with a 3 mm aluminum target, the interaction of the electrons with the window and the target produces X-rays (bremsstrahlung).

The effect of the X-rays produced by the accelerator is measured experimentally by using an X-ray monitor placed in front of the accelerator output as shows in Fig. 1. A 4 digits digital voltmeter is connected at the output of the monitor to visualize and record the voltage generated by the radiation.
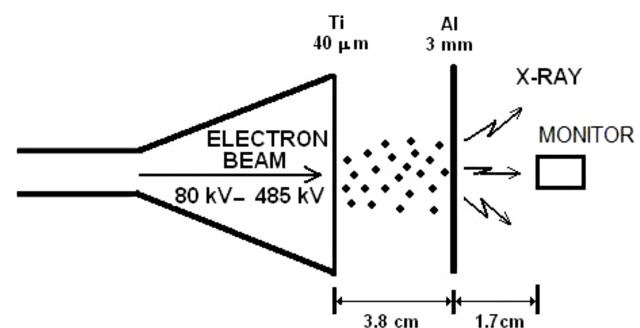

FIGURE 1. Setup used in the measurement of electrons and X-rays with a PIN diode detector.

The accelerating voltage and the beam current of the accelerator are varied accordingly in order to get the parametric graphs: the accelerating voltage is keep constant and the beam current is varied, afterwards the beam current is keep constant and the accelerating voltage is varied.

During the experiment, there was a serious uncertainty in the readings of the accelerating voltage at the terminal electrode in the accelerator; therefore an alternative spectroscopic technique was employed to verify the accelerating voltage. For higher voltages, a nuclear reaction could be used to verify the accelerating voltage.

3.1.   Verification of the Accelerating Voltage

The uncertainty in the digital readings of the accelerating voltage, when it was measured with an electrostatic generating voltmeter [High Voltage Engineering Corporation], was due to a declared non linearity in the low range of voltages, a big dependence in the sensitivity of the generating voltmeter with respect to the variations in tank gas pressure and temperature and the composition of the gas mixture inside the accelerator tank. Also a lack of calibration in the associated digital voltmeter was identified, therefore their readings were verified and corrected by means of a non invasive method [8] using an X-ray spectrometer with a lithium- drifted silicon detector, Si(Li), for low energies, from 85 keV to 280 keV, the main characteristics of the system are: cooled Si(Li) detector 4 mm diameter, 3 mm thickness, 185 eV resolution for the 5.89 keV, Fe-55 peak.

The spectrometry system is placed in front of the accelerator beam as shown in Fig. 2; in this verification, the distance from the electron beam output to the detector is 1m. The 3 mm thick aluminum target is placed at 3.8 cm from the Ti window and could be removed at will; when it is on, it only permits the pass of X-rays to the detector, stopping the pass of electrons.

The spectroscopy system is calibrated in energy with standard radiation sources before it is used; a data acquisition with a multichannel analyzer is made and the corresponding energy spectrum is obtained (see Fig. 3). The accelerating voltage is determined from the spectrum, considering the maximum energy point where the number of counts reaches cero; because high count rate conditions are present in these
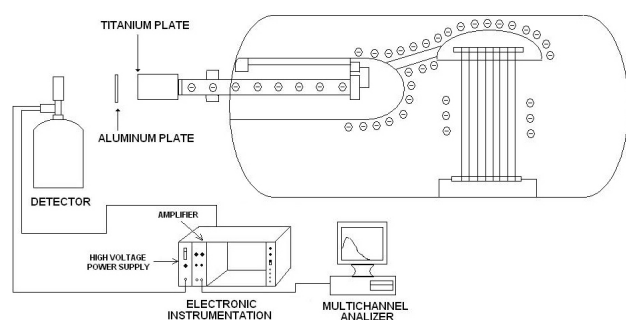

FIGURE 2. Setup used in the measurement of the X-rays energy with a spectroscopy system.
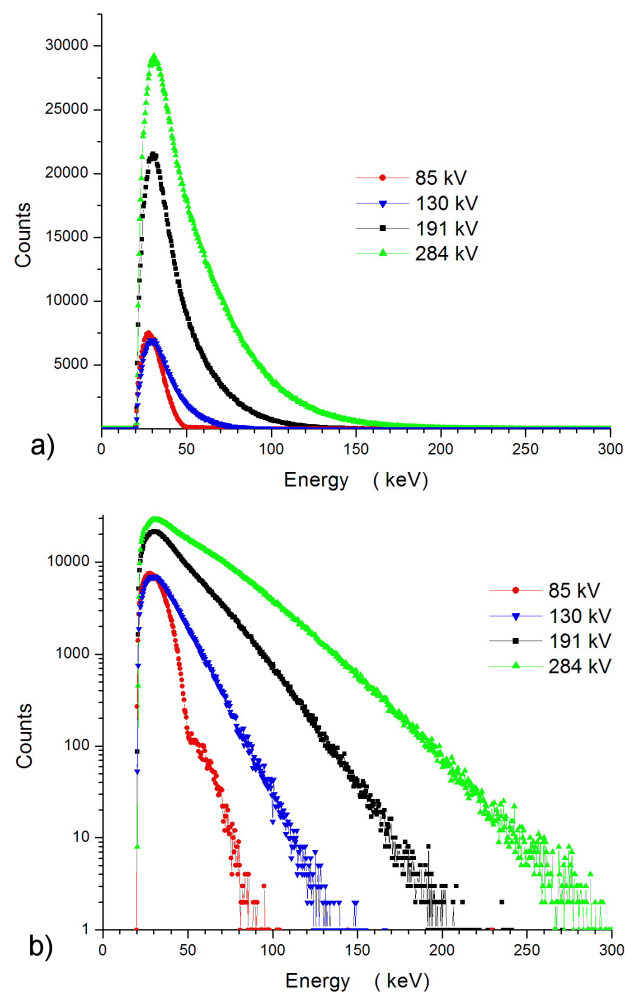

FIGURE 3. Energy spectra obtained with a Si(Li) detector.

measurements, pulse pile up effects are considered to determine the accelerating voltage according with Refs. 9 and 10. Finally the voltage value obtained from this method is compared with the voltage indicated in the digital display of the generating voltmeter, a correction factor was obtained for the considered range of accelerating voltages.

In the Fig. 3, the accelerating voltage corresponds in value to the end energy in the high energy side of the spectra, *i.e.* the spectrum for an accelerating voltage of 85 kV ends at an energy of 85 keV, as seen more clearly in the logarithmic view of Fig. 3b).

It is noticed that at high accelerating voltages the spectra start to spread from a single line, it is due to the lost of efficiency of the detector at high energies.

Trying to define better the spectra at higher energies, the same measurements were realized by using a gamma ray spectrometer with a high purity germanium detector, HPGe, for energies from 85 keV to 485 keV, see Fig. 4. The main characteristics of the system are: HPGe coaxial detector, 10 % relative efficiency, 43 mm diameter, 41 mm height, resolution 2.1 keV for the 1332.5 keV peak of Co-60.
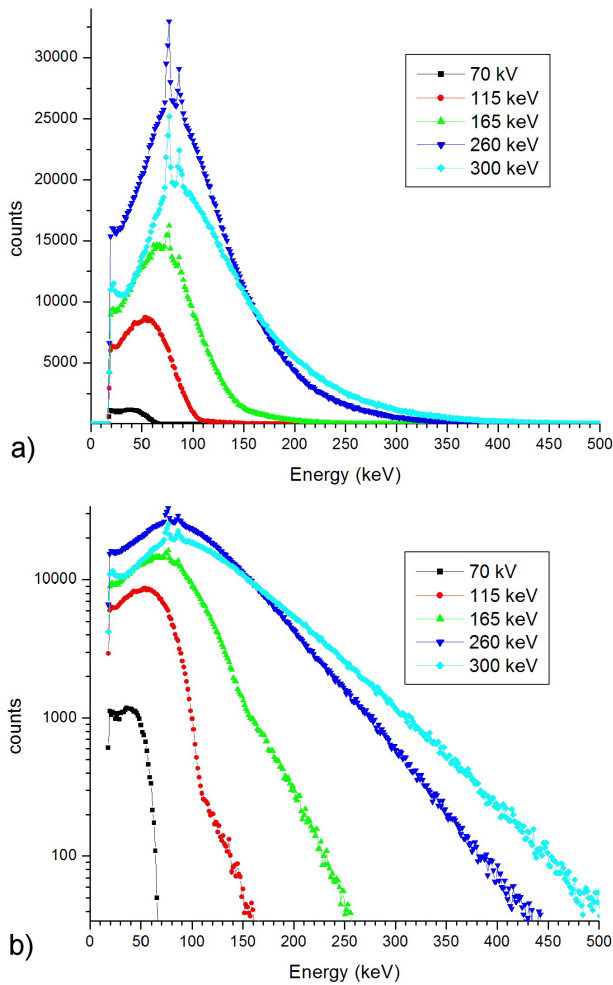
FIGURE 4. Energy spectra obtained with a HPGe detector.

FIGURE 5. Energy spectra obtained with a NaI(Tl) detector.

The spectra from Fig. 4 are better defined at high energies than in the former case but again some dispersion can be seen at higher energies. The correspondence between end energy and accelerating voltage remains valid, mainly if we observe the linear spectrum of Fig. 4a).

The two peaks at the low energy side are due to the fluorescence X-rays of the lead shield that was put near the detector to verify the energy calibration.

The same measurements were realized by using a gamma ray spectrometer with a 3.81×3.81 cm sodium iodine detector, NaI(Tl), see Fig. 5, in this case it was difficult to get a clear relationship between accelerating voltage and end energy at high energies.

4. Analysis of the Setup

An electron beam requires a minimum amount of energy to pass through a 40 μm titanium window; such energy can be calculated by means of the Continuous Slowing Down Approximation, CSDA. From the range graph [11] shown in the Fig. 6, the range can be obtained as:
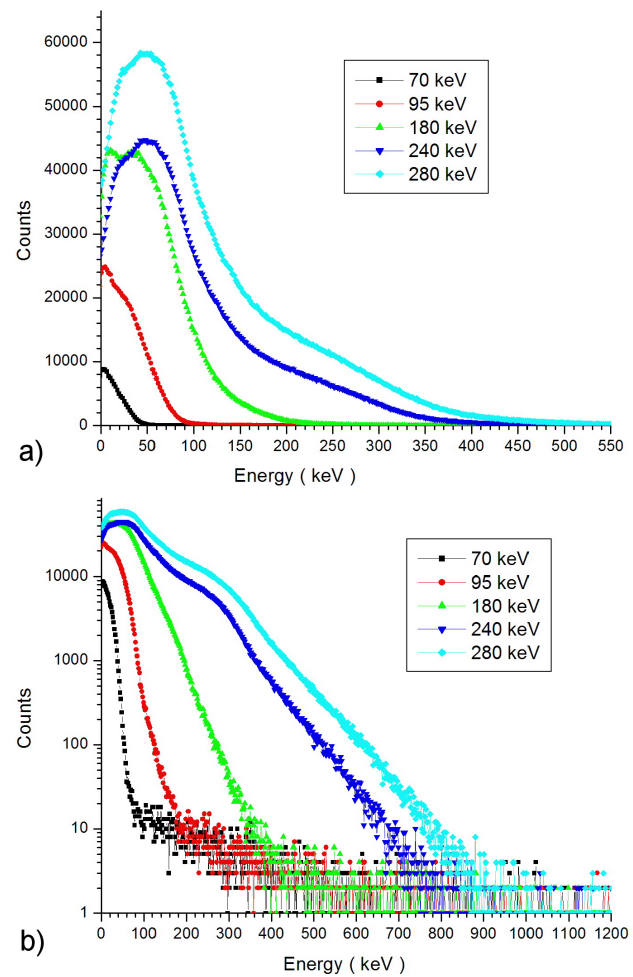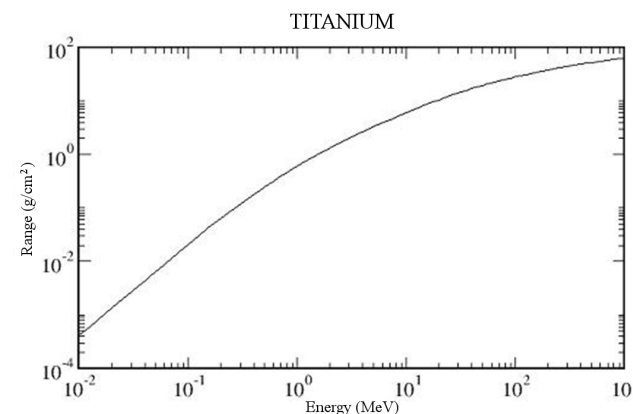
$$\text{range} = x \cdot \rho \qquad (2)$$

FIGURE 6. CSDA graph for electrons in titanium.

where: x is the thickness (cm) and ρ is the density of the material (g/cm^3).

The density for titanium is ρ = 4.507 g/cm^3, hence the range for the electrons through the 40 μm window is

0.0180 g/cm^2, then according to the graph in Fig. 6 the electrons require at least an energy of 90 keV to pass through the titanium window, this fact was verified experimentally.

When the accelerator is set to a fixed accelerating voltage, it is possible to estimate the energy of the electrons that can reach the aluminum plate, which is placed 3.8 cm apart from the window, by using the stopping power formula:

$$SP = \frac{\Delta E}{\rho\, x} \qquad (3)$$

where: SP is in (MeV·cm^2)/g , ΔE is the energy loss (MeV) of a particle when it passes through a material of thickness x.

For example, if the accelerating voltage is set at 500 kV, the maximum energy of the electrons emitted by the machine will be 500 keV. For this energy value, according to Fig. 7, the stopping power for titanium is 1.470 MeV·cm^2/gr [11] and the energy loss of the particle in the titanium window will be 26.50 keV. After crossing the titanium window the energy of the electrons will be 500 - 26.50 keV = 473.5 keV.

The stopping power in air for electrons with an energy of 473.5 keV is 1.809 MeV cm^2/gr [11], when it crosses 3.8 cm of air (ρ=1.3×10^{-3} g/cm^3) the energy loss is ΔE =8.94 keV. Therefore, the electrons reach the aluminum plate with an energy of 473.5 - 8.94 keV = 464.56 keV.

The thickness of the aluminum plate, x, required to stop all the electrons can be calculated with these parameters: ΔE=464.56 keV, ρ=2.70 g/cm^3 and SP=1.604 MeV·cm^2/gr, therefore, x=1.073 mm. This means that an aluminum plate with a thickness greater than 1.073 mm will stop the electrons with energies below 500 keV, only the X-rays produced by bremsstrahlung effect will reach the detector, thus, when the aluminum plate is placed in front of the accelerator all the electrons will be stopped and the voltage signal of the X-ray monitor will be produced only by the effect of the X-rays. If the aluminum plate were removed, the electrons could interact with the PIN diode and would produce a bigger voltage signal at the X-ray monitor output [12].
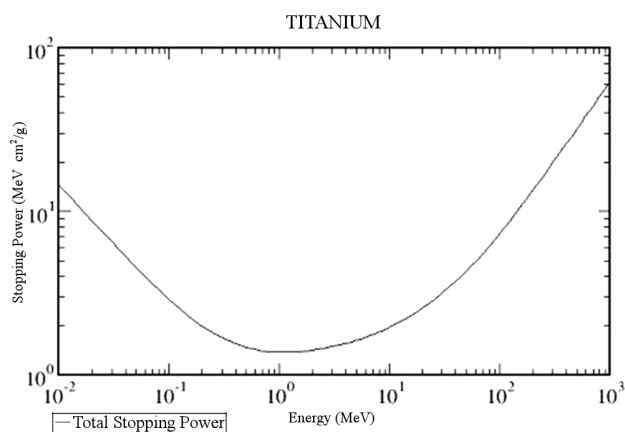
5. Measurements with the pin diode

The electric current (A/cm^2) produced by the X-rays inside a PIN diode detector is:

$$I_n = \frac{N_p\, e\, E_p}{w} \qquad (4)$$

where: e is the electron charge (C), and w is the energy required to produce an electron hole pair; the characteristic value for silicon is w = 3.6 eV at room temperature [13]. Therefore, comparing Eqs. (1) and (4), we see that the current generated in the diode is directly proportional to the intensity of X-rays:

$$I_n = \frac{I_x e}{w} \qquad (5)$$

A variation in the beam energy caused by a change in the accelerating voltage would produce a bigger change in the X-ray intensity and in the dose rate [7] if compared with a change in the beam current, and then the accuracy to set the accelerating voltage is critical in order to get a defined dose rate [14].

5.1. X-Ray Monitor

An OPF420 PIN diode was used for the detection of the X-rays generated in the accelerator, the active area of the diode is 1 mm^2 and its thickness is 150 μm. It was connected in photovoltaic mode (see Fig. 8), forming in this way an X-ray monitor. When a radiation beam interacts with the semiconductor material, it generates electron-hole pairs in the active region, thus an electric current will flow through the diode terminals. The detector current is converted to voltage in the first stage of the preamplifier. In the output stage, the voltage is amplified to obtain a total conversion gain of 240 mV/nA [15]. The X-ray monitor output is connected to a 4 digits digital voltmeter to get the reading of the voltage. The operational amplifiers used in the circuit must have a very low input bias current, low input offset voltage and low input offset current in order to minimize errors at the output, the LF441 operational amplifier was selected because it fulfills all these requirements.

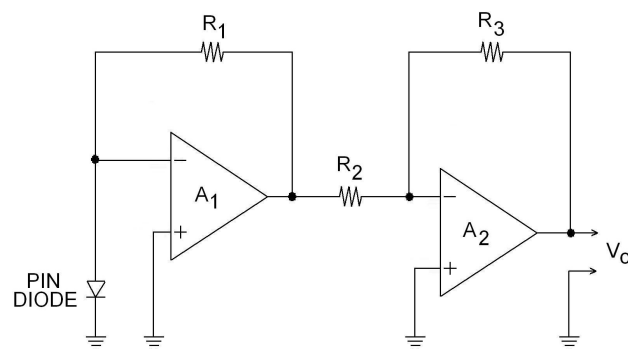FIGURE 7. Stopping power graph for electrons in titanium.

FIGURE 8. X-ray monitor formed by a PIN diode connected in photovoltaic mode and the amplifier section.
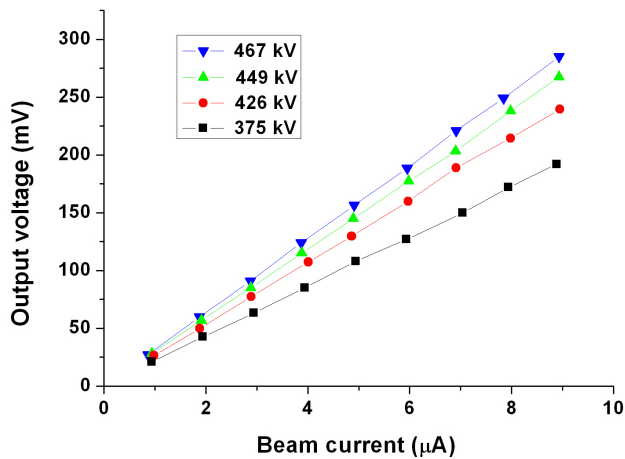
FIGURE 9. X-ray measurements with fixed accelerating voltage and different beam currents.
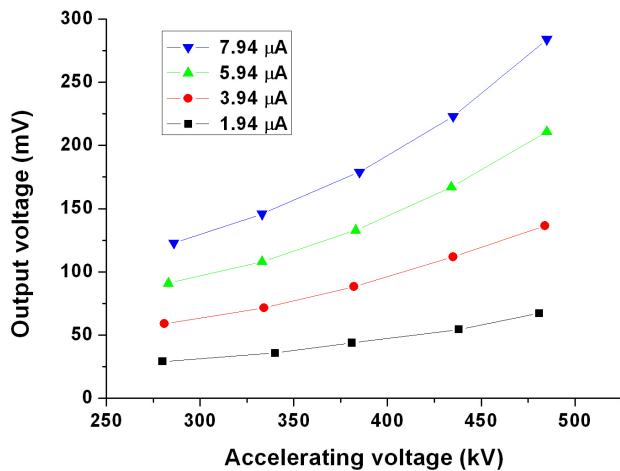

FIGURE 10. X-ray measurements for constant beam currents, varying the accelerating voltages.

5.2. Measurements of the X-Ray intensity

The output voltages of the X-ray monitor for fixed accelerating voltages and different beam currents are shown in Fig. 9, also the diode response when the beam currents were maintained constant and the accelerating voltages were varied are shown in Fig. 10. With these graphs the modeling of the response of the X-ray monitor can be performed.

5.3. Results on the Response of the PIN Diode Detector to the Different Beams Produced in the accelerator

Before any irradiation of the X-ray monitor at the accelerator, the offset voltage in the preamplifier output of Fig. 8 was -40 mV, this was due to the leakage current in the PIN diode and the own offset voltage of the operational amplifiers, this offset was removed by proper adjustment in the amplifiers. The accelerating voltage was fixed at 300 kV and the beam current to 2 μA, the Fig. 11 shows the response of the X-ray monitor to different conditions in the experiment: at t =10 s, the accelerator is turned on, with the titanium window and
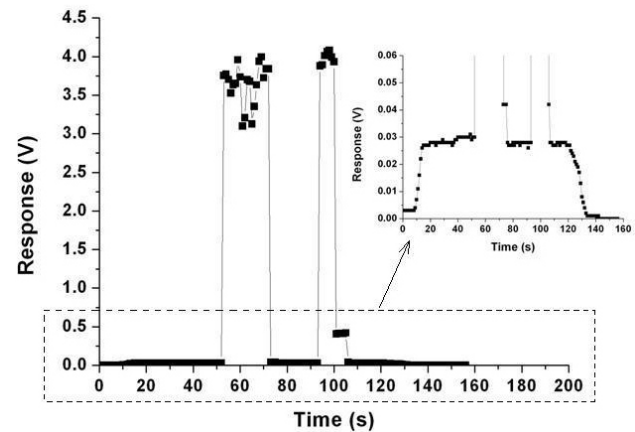

FIGURE 11. Output signal of the X-ray monitor for electrons and X-rays. The insert shows an enlarged view of the response of the monitor to the X-rays.

the aluminum plate put in the path between the beam and the monitor, the output voltage of the monitor increases to 28 mV, it corresponds to the detection of the X-rays produced in the interaction of the electrons with the window and target. When the aluminum plate is removed at t =55 s, the response goes to higher values as result of the interaction of the electrons with the detector, see more details in the Fig. 11, the further changes in the position of the aluminum plate are reflected in the response of the monitor, even a programmed reduction in the beam current by the operator is observed at t = 120 s before the shutting down of the accelerator.

6. Conclusions

The number of photons that an electron beam can produce by bremsstrahlung effect is approximately 0.5% of the total electrons at 60 kV and depending on the accelerating voltage, this number can increase up to 70% at 20 MV [16]. The accelerating voltage in an electron accelerator can be obtained by means of a measurement with a non invasive method in this case an spectroscopy system using Si-Li, GeHp and NaI(Tl) detectors [8-10].

The signal produced inside the PIN diode is related with the intensity of particles or photons that interact with the semiconductor. The PIN diode detector has the capability to detect both electrons and X-rays in the accelerator; consequently, the electrons generate a bigger output signal.

The response of the PIN diode monitor to the X-rays is as shown in the graphs of Fig. 9 and Fig. 10. The X-ray monitor can be used for the evaluation of the X-ray intensity of bremsstrahlung in electron accelerators in the range from 80 keV to 485 keV.

Acknowledgments

1. M. Stephan, D. Pospiech, R. Heidel, T. Hoffman, D. Voigt, and H. Dorschner. *Polymer Degradation and Stability* **90** (2005) 379.

2. O.N. Tretinnikov, S. Oggata, and Y. Ikada, *Polymer*. **39** (1998) 6115.

3. B. N. Turman, R. J. Kaye, and J.A. Jacobs, *Twenty-Fifth International Power Modulator Symposium and High Voltage Workshop*, Conference Record, (2002) 39.

4. J. McKeown, *IEEE Trans Nucl Sci.*, NS-32, (1985).

5. O. V. Chubarov, A. S. Alimov, and V. I. Shvedunov, *IEEE Trans Nucl Sci* **44** (1997).

6. G. Vázquez Polo, H. López Valdivia, and H. Carrasco Abrego, *X Congreso Nacional Sobre Dosimetría del Estado Sólido*, (Salazar Edo. de México, 1997).

7. F. J. Ramírez-Jiménez, *Nucl Instrum and Methods* **A609** (2009) 187.

8. M. C. Silva, S. B. Herdade, P. Lammoglia, P. R. Costa, and R. A. Terini, *Med Phys* **27** (2000).

9. K. Kudo, N. Takeda, T. Noguchi, H. Ohgaki, and T. Yamazaki, *IEEE Nuclear Science Symposium* **1** (1997) 742.

10. L. Wielopolski, and R. Gardner, *Nucl Instrum and Methods* **133** (1976) 303.

11. http://physics.nist.gov/PhysRefData/Star/Text/ESTAR.html

12. G. Knoll, "*Radiation Detection and Measurements*" Third Edition, (Ed. John Wiley and Sons, USA, 2000).

13. G. Bertolini, and A. Coche, "*Semiconductor Detectors*" (John Willey and Sons, Holland, 1968).

14. C. Ekdahl, *IEEE Trans. Plasma Sci.* **30-1** (2002) 254.

15. F. J. Ramírez-Jiménez, and M. A. Martínez H., *Am Inst Phys*, CP **724** (2004) 249.

16. S. C. Bushong, "*Radiation Science for Technologists*" (Fifth Edition, Ed. Mosby/Doymar, USA, 1995).